AIP | Applied Physics Letters

Effects of In profile on simulations of InGaN/GaN multi-quantum-well light-emitting diodes

Patrick M. McBride, Qimin Yan, and Chris G. Van de Walle

Citation: Applied Physics Letters **105**, 083507 (2014); doi: 10.1063/1.4894464
View online: http://dx.doi.org/10.1063/1.4894464
View Table of Contents: http://scitation.aip.org/content/aip/journal/apl/105/8?ver=pdfcov
Published by the AIP Publishing

Effects of In profile on simulations of InGaN/GaN multi-quantum-well light-emitting diodes

Patrick M. McBride,[1] Qimin Yan,[1,2] and Chris G. Van de Walle[1]
[1]*Materials Department, University of California, Santa Barbara, California 93106-5050, USA*
[2]*Molecular Foundry, Lawrence Berkeley National Laboratory, Berkeley, California 94720, USA*

(Received 16 April 2014; accepted 21 August 2014; published online 28 August 2014)

We investigate the impact of incorporating realistic In profiles in simulations of *c*-plane InGaN/GaN light-emitting diodes. Simulations based on a drift-diffusion model typically overestimate the onset voltage, but have usually been based on the assumption of ideal quantum wells with a square In profile. We demonstrate that more realistic profiles lead to significant modifications of current-density-versus-voltage characteristics, and explain the effects based on changes in the band diagram and carrier overlap. © *2014 AIP Publishing LLC*. [http://dx.doi.org/10.1063/1.4894464]

Light-emitting diodes (LEDs) based on group III-nitrides have come to the forefront of efficient lighting technologies. Current commercial devices are based on *c*-plane heterostructures, while semipolar and nonpolar devices are in development. The LEDs use multi-quantum-well structures with InGaN quantum wells (QWs) and GaN barriers. Device simulations can play an important role in designing and improving LED structures. Simulations using a semi-empirical drift-diffusion model have been used extensively,[1,2] but are often rightfully criticized because they typically produce current-density-versus-voltage curves that significantly differ from experiment. This is particularly evident in an overestimate of the turn-on voltage.

Ad hoc solutions have been proposed in order to improve the agreement with experiment. One approach has focused on the polarization fields that are present in InGaN *c*-plane QW structures due to the presence of spontaneous and piezoelectric polarization in the wurtzite structure.[3,4] The resulting quantum-confined Stark effect causes a reduction in the spatial overlap of electrons and holes, thereby reducing the internal quantum efficiency (IQE) of the device. A number of previous device simulation studies introduced an *ad hoc* reduction of the polarization fields (by as much as a factor of 2)[5–8] aimed at more closely fitting the experimental I-V curves. Justification for such an approach is lacking. There is no reason to believe that the widely used polarization constants of Bernardini and Fiorentini[9,10] are inaccurate, and no independent evidence for strong screening of the polarization fields has been produced.

Virtually, all simulations, however, have made the assumption that the InGaN/GaN interfaces are ideal and abrupt, and that the In content within the quantum well is constant, amounting to a square In profile within the QW. Experimental evidence is mounting that this square In profile is not a good description of the InGaN alloy. Atom-probe[11,12] and high resolution transmission electron microscopy[13,14] measurements of the In distribution in the multi-QW structure have shown that the In concentration does not change abruptly, but quite gradually, at the InGaN/GaN interfaces, and that in the thin QWs typically used in *c*-plane devices the In profile does not even reach a plateau. Furthermore, recent works have shown that alternate QW shapes can improve the device efficiencies.[7,15–17]

In this work, we systematically explore the effects of the In profile on the device characteristics of InGaN/GaN MQW LEDs. We demonstrate that deviations from the square profile can lead to significant changes in the current-density-versus-voltage curves, in particular, a lower turn-on voltage. These results indicate that an inaccurate description of the In profile, rather than deficiencies in materials parameters or descriptions of polarization fields, is to blame for failures to accurately model nitride LEDs in previous simulations. The work of Wu *et al.*[11] also investigated the effects of In distribution, but focused on the effects of lateral variations in the In concentration. While such variations may induce additional effects, what we are demonstrating in the present work is that the In profile along the growth direction by itself has a large impact on the device characteristics. Our analysis of band diagrams and electron-hole overlap allows us to identify the physical origins of the effect.

Our simulations are performed using the SiLENSe simulation software,[1,2] which implements a 1D semi-empirical drift-diffusion model to determine the current density and carrier densities. Quantum mechanical calculations are implemented on top of drift-diffusion simulations to obtain electron-hole wavefunctions and overlap integrals.[18] The simulated LED device, shown in Fig. 1, includes a 0.3–μm *n*-type GaN layer ($N_D = 7 \times 10^{18}\,\mathrm{cm}^{-3}$) and an active region on top. This active region is capped off with a 10-nm *p*-type GaN barrier layer ($N_A = 6 \times 10^{18}\,\mathrm{cm}^{-3}$), a 10-nm *p*-type $Al_{0.2}Ga_{0.8}N$ EBL ($N_A = 3 \times 10^{19}\,\mathrm{cm}^{-3}$), and finally a 0.2–$\mu$m *p*-type GaN capping layer ($N_A = 2 \times 10^{19}\,\mathrm{cm}^{-3}$). Here, N_D and N_A represent the donor and acceptor dopant concentrations. The active region consists of three 3-nm $In_{0.2}Ga_{0.8}N$ QWs separated by 10-nm GaN barriers. Unintentional *n*-doping concentration of $2 \times 10^{17}\,\mathrm{cm}^{-3}$ was assumed throughout the active region, and the three QWs all have the same width and In profile. Three different In profiles are considered, as illustrated in Fig. 2: square, parabolic, and triangular, all with the same peak In concentration.

Figure 3(a) shows results for current-density-versus-voltage curves resulting from our simulation using the three different In profiles. The conventional square In profile gives

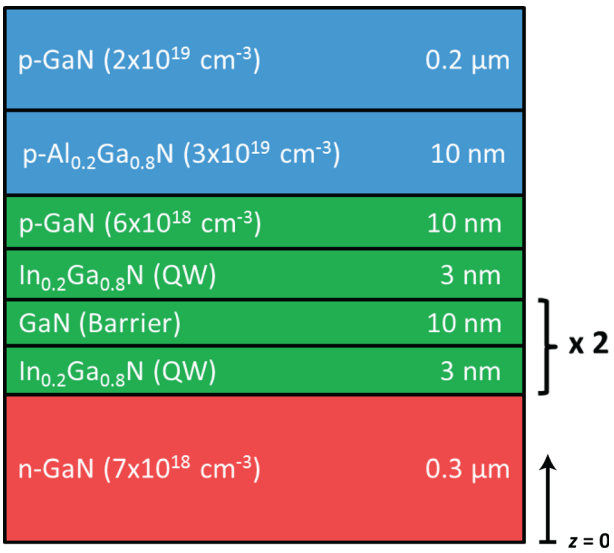

FIG. 1. Schematic of the layer structure for the simulated nitride LED (not to scale). Distances in Figs. 3 and 4 are measured from the bottom of the *n*-type layer as indicated by the label $z = 0$.

rise to a turn-on voltage significantly higher than experimentally measured[19,20] (we define the turn-on voltage to be the voltage at a current density of 10 A/cm^2). We observe that a change in the In profile to reflect more realistic In distributions in the QW leads to sizeable changes in the J-V curves, particularly a reduction in the turn-on voltage from 3.8 V for a square well to 3.2 V for a triangular well.

To provide further insight into the mechanisms at play, we plotted the band diagrams for the three In profiles in Fig. 3(b). When the QW shape changes from square to parabolic to triangular the hole barrier height decreases towards the *p*-side. This promotes hole injection into the QWs, thereby increasing the number of available carriers for recombination within the QWs.

The current density at a certain bias voltage is related to the total electron-hole recombination rate (both radiative and nonradiative) in the InGaN QWs. These recombination rates depend on the overlap of electron and hole wavefunctions, specifically, they are proportional to the square of the wavefunction overlap integral: $|F|^2 = |\langle\psi_e|\psi_h\rangle|^2$(Ref. 21). Our calculations show that the change in In profile has a major effect on the electron-hole overlap: going from a square to a triangular profile leads to an increase in $|F|^2$ from 13.9% to 46.3%, as shown in Fig. 4.

The indium gradient in the parabolic and triangular QWs leads to two notable effects:[15] (1) a reduction in the

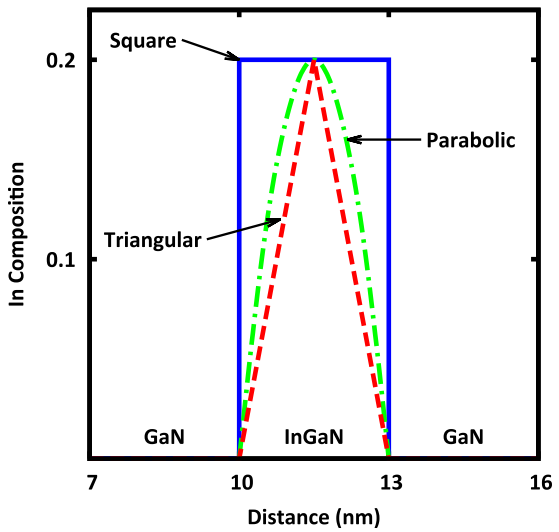

FIG. 2. In composition in the InGaN QW as a function of coordinate along the growth direction, for the three different cases considered: square, parabolic, and triangular. Distances are measured from the left edge of the GaN barrier.

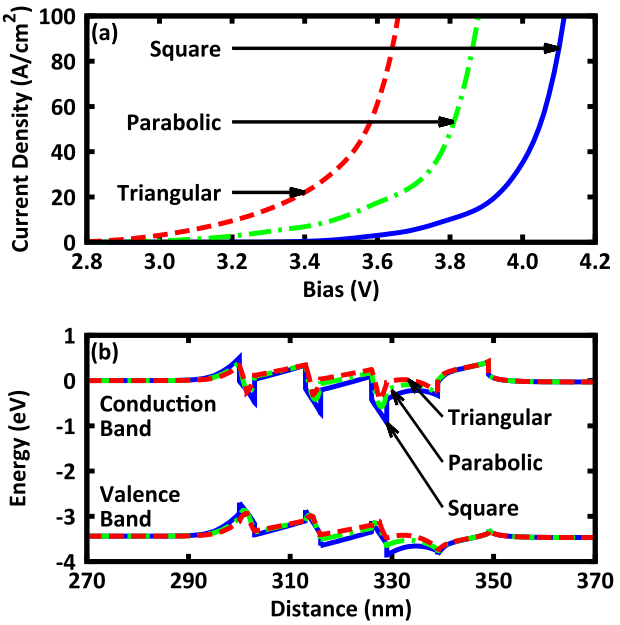

FIG. 3. (a) *J-V* characteristic for the $In_xGa_{1-x}N$/GaN LEDs with square, parabolic, and triangular In profiles in the QWs. The corresponding turn-on voltages are 3.8 V, 3.5 V, and 3.2 V, respectively. (b) Band diagrams for the $In_xGa_{1-x}N$/GaN LEDs with different In profiles, under flat-band conditions (bias = 3.35 V). Distances are measured from the bottom of the *n*-type layer as indicated in Fig. 1.

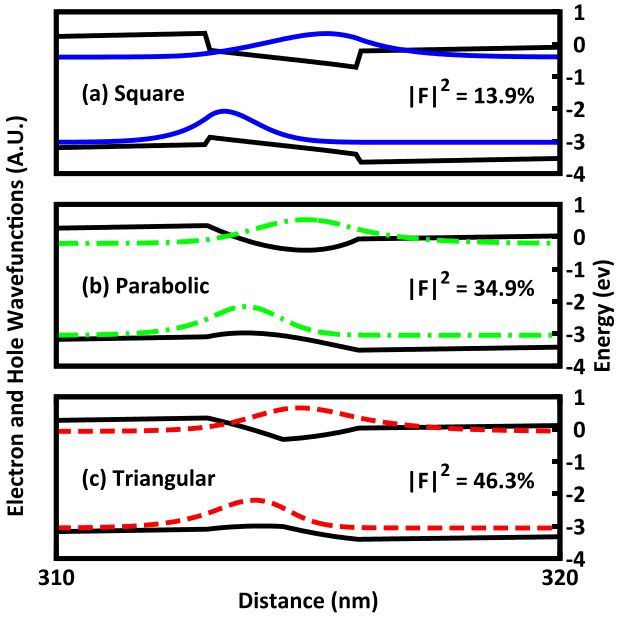

FIG. 4. Electron and heavy-hole wavefunctions in the central QW for the $In_{0.2}Ga_{0.8}N$/GaN multi-QW structures with (a) square, (b) parabolic, and (c) triangular In profiles. Distances correspond to those in Fig. 3(b).

piezoelectric field on the outer edge of the QW and (2) the creation of a potential extremum in the center of the well. The first effect reduces the quantum-confined Stark effect across the QW, thereby increasing the electron-hole overlap. The second effect pulls the electrons and holes into the same, narrow region of the QW, which increases the driving force for recombination. Together, these two effects lead to a significant increase of the total recombination rate.

Our conclusions about the physical mechanisms are confirmed by simulations we performed for nonpolar QWs. There, the different QW profiles have little or no effect on the onset voltage, which stays around 2.9 V. This confirms that the variations in In profile affect the onset voltage mainly through their effect on polarization fields.

Note that in the SiLENSe code the current density is calculated based on the carrier distribution in the QWs without inclusion of quantum-mechanical effects; the wavefunction overlap integral is therefore not directly used. In spite of this, the obtained current density from SiLENSe simulations can still qualitatively represent the effect of the distribution of carriers and their overlap on the *J-V* characteristic. Less abrupt interfacial transitions lead to more gradual piezoelectric fields that are small at the edges of the QW and peak at the center. This reduces the quasi-electrostatic separation of the electrons and holes in the QW, allowing for greater recombination rates as their carrier densities overlap.

As noted in the introduction, previous attempts to improve the agreement of simulations and experiment employed an *ad hoc* reduction of polarization fields.[5–8] As a check, we also implemented this approach in our simulations, by reducing the bulk piezoelectric and spontaneous polarization constants.[10] We find that a reduction in polarization constants from 100% to 50% of their full values indeed reduces the turn-on voltage, from 3.8 V to 3.1 V. However, as noted earlier, there is no independent justification for such an arbitrary modification of these values. In contrast, deviations from a square In profile are well documented and our work shows inclusion of non-abrupt profiles in the simulations leads to a significant decrease in onset voltage.

In summary, we have studied the effects of indium profiles on the performance of InGaN/GaN multi-QW LED devices. The abrupt, square In profile commonly assumed in simulations leads to turn-on voltages much greater than experimental values (or, alternatively, a current density much lower than the experiment at a given voltage). Simulations using more realistic In profiles (in particular, without abrupt interfacial transitions) lead to current-density-versus-voltage curves in much closer agreement with the experiment. The improvement can be attributed to changes in internal fields and electron-hole overlaps. Our work emphasizes the importance of using accurate information about In distributions in quantum wells when performing simulations, highlighting the need for advanced electron microscopy and atom-probe techniques.

We thank Sergey Karpov for discussions and support with SiLENSe. P.M.M. gratefully acknowledges support of a Bonderson Fellowship and of UCSB's Institute for Energy Efficiency Holbrook Foundation Fellowship. Q.Y. was supported by the UCSB Solid State Lighting and Energy Center. C.G.V.dW. was supported by the U.S. Department of Energy, Office of Basic Energy Sciences, under Award # DE-SC0010689. Computational resources were provided by the Center for Scientific Computing at the CNSI and MRL (an NSF MRSEC, DMR-1121053), (NSF CNS-0960316), and by NERSC which is supported by the National Energy Research Scientific Computing Center (NERSC) which is a DOE Office of Science User Facility supported by the Office of Science of the U.S. Department of Energy under Contract No. DE-AC02-05CH11231.

[1]K. A. Bulashevich, O. V. Khokhlev, I. Y. Evstratov, and S. Y. Karpov, Proc. SPIE **8278**, 827819 (2012).
[2]S. Y. Karpov, Proc. SPIE **7939**, 79391C (2011).
[3]D. F. Feezell, M. C. Schmidt, S. P. DenBaars, and S. Nakamura, MRS Bull. **34**, 318 (2009).
[4]A. E. Romanov, T. J. Baker, S. Nakamura, and J. Speck, J. Appl. Phys. **100**, 023522 (2006).
[5]Y.-K. Kuo, J.-Y. Chang, and M.-C. Tsai, Opt. Lett. **35**, 3285 (2010).
[6]C. H. Wang, S. P. Chang, P. H. Ku, J. C. Li, Y. P. Lan, C. C. Lin, H. C. Yang, H. C. Kuo, T. C. Lu, S. C. Wang, and C. Y. Chang, Appl. Phys. Lett. **99**, 171106 (2011).
[7]T.-H. Wang, J.-Y. Chang, M.-C. Tsai, and Y.-K. Kuo, Proc. SPIE **7954**, 79541F (2011).
[8]U. Özgür, X. Ni, J. Lee, S. Liu, S. Okur, V. Avrutin, A. Matulionis, and H. Morkoç, Semicond. Sci. Technol. **26**, 014022 (2011).
[9]F. Bernardini and V. Fiorentini, Phys. Status Solidi B **216**, 391 (1999).
[10]F. Bernardini, V. Fiorentini, and D. Vanderbilt, Phys. Rev. B **63**, 193201 (2001).
[11]Y.-R. Wu, R. Shivaraman, K.-C. Wang, and J. S. Speck, Appl. Phys. Lett. **101**, 083505 (2012).
[12]S. E. Bennett, T. M. Smeeton, D. W. Saxey, G. D. Smith, S. E. Hooper, J. Heffernan, C. J. Humphreys, and R. A. Oliver, J. Appl. Phys. **111**, 053508 (2012).
[13]C. Kisielowski, Z. Liliental-Weber, and S. Nakamura, Jpn. J. Appl. Phys. **36**, 6932 (1997).
[14]T. P. Bartel and C. Kisielowski, Ultramicroscopy **108**, 1420 (2008).
[15]Z. Yang, R. Li, Q. Wei, T. Yu, Y. Zhang, W. Chen, and X. Hu, Appl. Phys. Lett. **94**, 061120 (2009).
[16]S.-H. Han, D.-Y. Lee, H.-W. Shim, G.-C. Kim, Y. S. Kim, S.-T. Kim, S.-J. Lee, C.-Y. Cho, and S.-J. Park, J. Phys. D **43**, 354004 (2010).
[17]R.-M. Lin, M.-J. Lai, L.-B. Chang, C.-H. Huang, and C.-H. Chen, Int. J. Photoenergy **2012**, 1–5.
[18]*SiLENSe Physics Summary v5.2* (2011).
[19]S.-H. Han, D.-Y. Lee, S.-J. Lee, C.-Y. Cho, M.-K. Kwon, S. P. Lee, D. Y. Noh, D.-J. Kim, Y. C. Kim, and S.-J. Park, Appl. Phys. Lett. **94**, 231123 (2009).
[20]W. Lee, M.-H. Kim, D. Zhu, A. N. Noemaun, J. K. Kim, and E. F. Schubert, J. Appl. Phys. **107**, 63102 (2010).
[21]E. Kioupakis, Q. Yan, and C. G. Van de Walle, Appl. Phys. Lett. **101**, 231107 (2012).